Wearable Stimulator for Upper and Lower Limb Somatotopic Sensory Feedback Restoration

Roberto Paolini, Riccardo Collu, Laura Tullio, Andrea Demofonti, *Member, IEEE*, Alessia Scarpelli, Francesca Cordella, *Member, IEEE*, Massimo Barbaro, *Senior Member, IEEE*, and Loredana Zollo, *Senior Member, IEEE*

***Abstract*—Neuroprostheses capable of providing Somatotopic Sensory Feedback (SSF) enables the restoration of tactile sensations in amputees, thereby enhancing prosthesis embodiment, object manipulation, balance and walking stability. Transcutaneous Electrical Nerve Stimulation (TENS) represents a primary non-invasive technique for eliciting somatotopic sensations. Devices commonly used to evaluate the effectiveness of TENS stimulation are often bulky and main powered. However, current portable TENS devices frequently fall short of key functional requirements, particularly in terms of stimulation parameter ranges that are insufficient to reliably evoke somatotopic sensations in either upper and lower limb applications. Moreover, they typically do not support real-time independent channels programming and wireless communication. This work introduces a compact, wearable stimulator, including its external casing, with a total weight of 64 g and dimensions of 70 × 40 × 35 mm, designed to deliver SSF in both upper and lower limb applications. The device was validated through bench testing and human trials involving 20 healthy participants, by comparing the intensity, qualitative characteristics, and referred area of the elicited sensations with those produced by a benchmark. The stimulator reliably delivered the required parameters on a skin-like capacitive-resistive load and elicited somatotopic sensations consistent with the benchmark device and prior somatotopic feedback studies. The proposed stimulator provides non-invasive somatotopic sensory feedback for both upper and lower limbs. Its portability and modular design address key limitations of current commercial and research-grade TENS systems, enabling future studies on the functional benefits of sensory feedback in prosthetic control.**

***Index Terms*—Electrical stimulation, TENS, somatotopic sensory feedback, wearable stimulator.**

I. Introduction

SOMATOTOPIC Sensory Feedback (SSF) improves embodiment and user acceptance of upper and lower limb prostheses by integrating sensory information into the user's internal sensorimotor models [1], [2]. By employing a SSF-integrated neuroprosthesis, amputees regain the ability to perceive tactile sensations directly in the missing limb [3], [4], [5], [6], [7]. This restoration facilitates discrimination of object properties, such as shape and texture, thereby enhancing performance in manipulation tasks [8], [9]. It also contributes to improved postural stability, gait speed, and balance, ultimately reducing fall risk [10], [11]. These effects are achieved by delivering charge-balanced current pulses to the residual peripheral nerves [12], via both invasive and non-invasive techniques [13], [14].

Although less selective than invasive approaches [15], Transcutaneous Electrical Nerve Stimulation (TENS) avoids surgical procedures and long-term complications, thereby enabling wider applicability of SSF in amputee populations [11], [16]. Prior studies have investigated the modulation of TENS waveform parameters to evoke distinct sensory qualities and intensities in both upper [9], [13], [17], [18], [19], [20] and lower limb [16], [21], [22], [23], [24].

These studies established optimal ranges and resolutions for Pulse Amplitude (PA), Pulse Width (PW), and Pulse Frequency (PF) modulation, reliably eliciting distinguishable tactile sensations in both able-bodied and amputee subjects. Notably, these investigations have shown that PW and PF share similar modulation trends across both regions (i.e., PW = 20:20:500 μs and PF = 20:20:500 Hz). However, PA requirements diverge significantly: while stimulation currents up to 3 mA with fine resolution (i.e., 0.1 mA) are typically sufficient for the upper limb, lower limb applications often demand higher current levels, up to 10 mA, but tolerate coarser resolution (i.e., 0.5 mA). The "Stimulation requirements" column in Table I summarizes the reported modulation ranges and resolutions for each stimulation parameter, integrating specifications derived from both upper and lower limb applications found in the literature.

Most of these studies employed commercial benchtop stimulators such as the STG4008 (Multichannel System MCS GmbH,

Received 13 June 2025; revised 2 August 2025; accepted 24 August 2025. Date of publication 9 September 2025; date of current version 30 January 2026. This work was supported in part by the European Union's Horizon 2020 Research and Innovation Program (SOMA Project) under Grant 899822, in part by the National Institute for Insurance against Accidents at Work (INAIL) Prosthetic Center with BioInterNect (CUP: E57G23000280005), and in part by the European Union's Horizon Europe Research and Innovation Program under Grant 101070328 (BioMeld). This paper was recommended by Associate Editor S. J. A. Majerus. *(Corresponding author: Roberto Paolini.)*

Roberto Paolini, Laura Tullio, Andrea Demofonti, Alessia Scarpelli, Francesca Cordella, and Loredana Zollo are with the Unit of Advanced Robotics and Human-Centred Technologies, Università Campus Bio-Medico di Roma, 00128 Rome, Italy (e-mail: r.paolini@unicampus.it).

Riccardo Collu and Massimo Barbaro are with the Department of Electrical and Electronics Engineering, University of Cagliari, Piazza D'Armi, 09123 Cagliari, Italy.

Color versions of one or more figures in this article are available at https://doi.org/10.1109/TBCAS.2025.3607203.

Digital Object Identifier 10.1109/TBCAS.2025.3607203

TABLE I
COMPARISON OF KEY STIMULATION FEATURES IN COMMERCIAL AND RESEARCH-GRADE TENS DEVICES

Reference	Trout et al. [35]	Wang et al. [29]	RehaMove3 [30]	Mereu et al. [36]	**Stimulation Requirements**
Upper limb	Yes	Yes	No	Yes	Yes
Lower limb	No	Yes	Yes	No	Yes
PA [mA]	-:-:6	0:0.1:10	0:0.5:130	0:0.02:5	0.1:0.1:10
PF [Hz]	1:-:250	0:1:1000 one active channel	10:2:500	100:-:500	20:20:500
PW [us]	N.D.	50:10:450	10:1:65520	100:-:600	20:20:500
VC [V]	± 150	80	150	± 36	/
Channels number	6	6	4	8	/

Reutlingen, DE) [8], [17], [21], [23], [25], [26], Master 9 (Iso-Flex, A.M.P.I. Company, Jerusalem, IL) [27], DS5/DS3 (Digitimer, Welwyn Garden City, UK) [3], [28], or Rehastim (HASOMED GmbH, Magdebur, DE) [4].

While these platforms enable precise waveform delivery, their large form factor and dependence on mains power limit their use in real-world, mobile applications.

To further investigate the advantages of SSF in upper and lower limb prosthetic control, the use of a wearable stimulator is essential to enable participants to dynamically perform activities of daily living (e.g., grasping and handling objects, walking on a ramp) in unstructured environments, offering a level of mobility that commercial benchtop TENS stimulators are unable to provide [1].

According to the literature, as reported in Table I, the portable device developed by Wang [29] is the only system capable of delivering SSF stimulation to both the upper and lower limbs.

The device offers appropriate stimulation parameters for both scenarios over six channels with an 80 V Voltage Compliance (VC). Biphasic waveforms are generated using a voltage-controlled current stimulation stage enabled by a monopolar power supply and an H-bridge. A key limitation of this system lies in its single current source architecture, which, through multiplexing, prevents true parallel stimulation and imposes a fixed pulse frequency across all active channels.

The use of at least two stimulation channels with independently configurable parameters is essential for eliciting more complex somatotopic feedback across a broader range of areas, thereby enhancing the representation of the perceived sensations [17], [26].

Other portable stimulation devices described in the literature or available on the market are equipped with stimulation parameters that are optimized for only one of the two target limbs. One commercial example is the RehaMove3 (HASOMED GmbH, Magdebur, DE) [30], a portable and compact device that has been utilized in several SSF studies [31], [32].

It features three stimulation channels and a sufficiently high VC to ensure the ± 10 mA current required for lower limb SSF scenario [33], [34]. Although it is possible to program the stimulation parameters in real time, the device needs wired communication and the coarse pulse amplitude resolution (0.5 mA) is unsuitable for upper limb applications [18].

In the literature, there are various wearable SSF current stimulation devices that have been at least validated on healthy participants.

Trout et al. [35] developed a multi-channel stimulator based on a Howland bidirectional current supply architecture. The system is powered by a voltage booster that elevates the 12 V battery pack output to over 150 V, thereby ensuring a high VC. However, real-time programming of stimulation parameters requires a wired connection, and the device is limited to a maximum PA of 6 mA, which is typically undersized for lower limb stimulation [24].

Mereu et al. [36] developed a wearable stimulation device featuring an external transmitter and an inductive powered current stimulation board. The stimulator is designed to acquire data from force sensors, process them using an encoding algorithm, and transmit the results directly to the front end via Bluetooth communication. By coupling the commercial stimulator RHS2116 (INTAN Technologies, Los Angeles, CA, USA) with a current mirror, powered by a voltage booster, the stimulation stage can generate currents up to 5 mA with a VC of ±36 V. Although the device supports real-time modulation of stimulation parameters across up to eight channels, its voltage compliance remains insufficient to reliably deliver the current levels required for effective lower-limb stimulation.

To the best of authors' knowledge, no existing wearable TENS system concurrently supports real-time wireless programming of multiple independently controlled channels for both upper and lower limb SSF.

To address these limitations, this work presents a compact, wearable stimulator that incorporates all the necessary features for effective somatotopic sensory feedback delivery across both upper and lower limbs. Designing a multipurpose stimulator also yields several translational benefits. A single, standardized hardware platform helps reduce manufacturing and maintenance costs and extends the applicability of the device to a broader target population. Furthermore, having a system capable of stimulating both upper and lower limbs allows its use in individuals with multi-limb amputations, offering a more versatile solution for clinical and at-home applications.

The novel device integrates (i) high voltage compliance suitable for both upper and lower limb stimulation, (ii) multiple independently programmable channels, (iii) real-time wireless control, and (iv) a user-friendly graphical interface.

Preliminary bench tests were conducted to validate the functionality of the device and assess its performance relative to a benchmark.

Finally, tests on healthy participants are conducted to validate the device ability to elicit sensations in both the upper and lower limbs.

The paper is structured as follows: Section II outlines the design requirements, the developed hardware and software components, and the experimental setup and protocol used for both benchtop and human validations. Section III presents the key results from both experimental trials. Finally, Section V discusses the performance of the proposed stimulator and suggests potential directions for future development of the presented work.

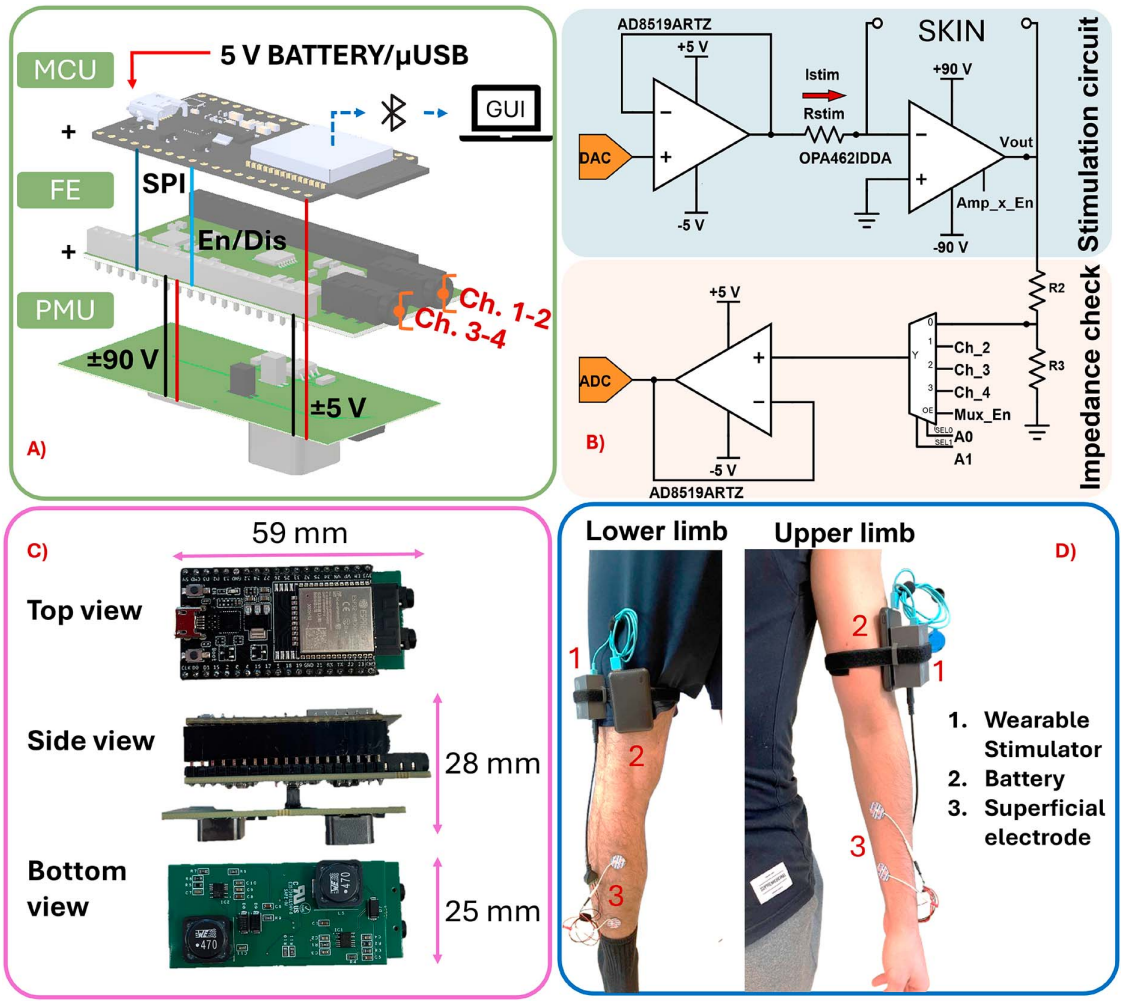

Fig. 1. (A) Exploded view of the wearable stimulator illustrating the three main modules: the Microcontroller Unit (MCU) is responsible for configuring the stimulation of the four Front-End (FE) channels via Serial Peripheral Interface (SPI) communication, and for managing the Enable/Disable (En/Dis) line to selectively power the multiplexer and the high-voltage operational amplifiers of each stimulation channel, thereby optimizing overall energy consumption; the FE modules that generate stimulation signals; and the power management unit (PMU) which converts the battery pack 5 V output to ±90 V, providing the necessary voltage compliance (VC) for effective skin stimulation. (B) Circuit schematic of one stimulation channel (Channel 1), including the impedance check circuit, enabling real-time verification of electrode-skin contact quality. (C) Top, side and bottom view of the assembled wearable stimulator printed circuit board. (D) Photos of the wearable stimulator and battery system applied to both lower and upper limbs.

II. Method

A. Hardware and Software Description

A custom wearable stimulator was developed to provide SSF via TENS to both upper and lower limbs. Stimulation parameters, including operational ranges and modulation resolution, were defined according to values reported in prior literature (Table I):

1) Wearable stimulator design: The stimulator, shown in Fig. 1, is implemented as a compact stacked architecture measuring 70 × 40 × 35 mm (L × W × H) and weighing 64 g, including the 3D-printed case. To ensure full wearability, it is powered by a 5 V, 5000 mAh rechargeable battery (100 g, 98 × 65 × 16 mm).

The system comprises two custom-designed printed circuit boards (PCBs) and a commercially available microcontroller unit (MCU). The system design separates the Power Management Unit (PMU) and the stimulation front end (FE), making the device modular and easily customizable regarding voltage compliance and stimulation current characteristics. Each PCB is a two-layer board with the same 59 mm x 28 mm dimensions, designed to be mounted on MCU, the ESP32-WROOM-32UE (Espressif System, Shanghai, CN). This dual-core, 32-bit microprocessor includes a built-in Bluetooth module and USB peripheral.

The PMU PCB is placed at the bottom of the stack. It generates the required supply voltages for the stimulation front end. The PMU includes two booster circuits based on a LT8365 (Analog Devices, Wilmington, MA, USA) switching voltage regulator and a voltage-inverting circuit. Using a MAX889RESA (Maxin Integrated, San Jose, CA, USA), the voltage-inverting circuit generates a -5 V supply, delivering 200

mA with a quiescent current of 2 mA, allowing a higher current with respect to the first prototype [34].

The LT8365 is employed in two distinct circuits. The first circuit utilizes the boosting feature to generate a + 90 V voltage supply from the 5 V input, with a maximum current of 66 mA delivered to the load. The second circuit uses the inverting feature to produce a -90 V voltage supply from the 5 V input. The power management module ensures high voltage compliance ($\pm$90 V), designed to support a maximum current of 18 mA for a load of 5 $k\Omega$, allowing coverage of the ranges of skin-electrode impedance reported in literature [33].

The FE unit PCB is positioned in the middle of the stack and receives both the high-voltage bipolar supply and the -5 V from the PMU and the 5 V supply from the MCU. It hosts the LTC2664 (Analog Devices, Wilmington, MA, USA), a 4-channel, 16-bit bipolar digital-to-analog converter (DAC), which controls the four stimulation channels.

Each output channel consists of a voltage-programmable voltage-to-current converter that delivers current to the load via two amplifiers: a low-voltage, rail-to-rail amplifier AD8519ARTZ (Analog Devices, Wilmington, MA, USA) and a high-voltage amplifier OPA462IDDA (Texas Instruments, Dallas, TX, USA).

To ensure proper load stimulation, the OPA462IDDA adjusts its output voltage within the wide range allowed by the $\pm$90 V supply. The OPA462IDDA provides a slew rate of 32 $\frac{V}{\mu s}$, delivering a maximum output current of about 45 mA.

The MCU uses the SPI protocol to program the DAC, enabling users to activate or deactivate any of the four channels. The low-voltage amplifier serves as a buffer to sink or source the stimulation current, which is set by the DAC output voltage and the resistor Rstim.

The load requiring stimulation is connected in feedback to the high-voltage amplifier, ensuring the desired current (Istim) flows as described in Fig. 1. This configuration ensures load-independent current delivery, allowing precise control of injected charge during biphasic stimulation [37], [38].

In biphasic stimulation, the injected charge (Q) is determined as follows:

$$\mathrm{Q} = \mathrm{Istim} \times \mathrm{PW}. \tag{1}$$

The LTC2664 DAC features an internal reference voltage, which can be programmed within the range of $\pm$2.5 V to $\pm$5 V. This allows for a current resolution of 381 nA in the 0-12.5 mA range and 762 nA in the 12.5-18 mA range. The DAC supports a maximum output of 2 ksps, which guarantees the required temporal resolution of 20 us.

The FE integrates an impedance sensing circuit capable of detecting loss of contact between the electrodes and the skin surface. The output voltage (Vout) of the OPA462IDDA, is continuously monitored by the ESP32 12-bit built-in analog-to-digital converter (ADC). Since the ADC is limited to measuring voltages in the range of 0 to 3.6 V, a 30 ratio voltage divider (R1 and R2) is implemented to scale the voltage down to fit within the measurable range. The scaled signal is routed through a multiplexer, enabling the selection of the channel to be monitored. Subsequently, a buffer isolates the sensing circuit from the ADC.

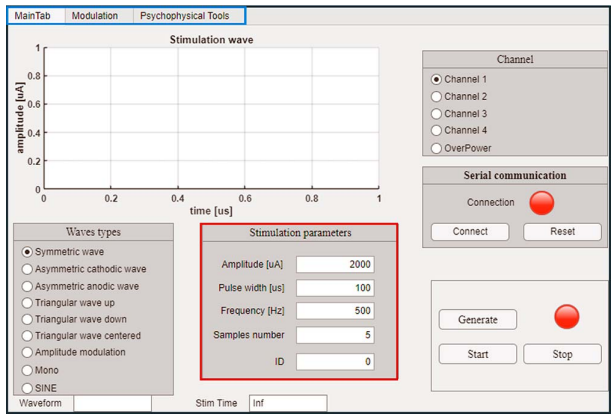

Fig. 2. Graphical interface main windows. This panel allows for the initialization of Bluetooth communication and the configuration of the primary stimulation parameters. In the upper left section of the window, users can access two additional panels: Modulation and Psychophysical Tools.

2) User interface: The graphical user interface (GUI) shown in Fig. 2 was developed using the MATLAB 2023 App Designer tool (MathWorks, Natick, MA, USA) and was designed to control the proposed stimulator.

It is based on three different windows that allow the management and modification of the main stimulation parameters, stimulus modulation algorithms, and psychophysical methods to search for stimulation thresholds.

The main window has been designed to initialize the communication with the portable device and modify the main stimulation parameters in terms of amplitude, frequency, pulse width, and type of stimulation waveform. The interface allow the selection of four different preset waveforms of monophasic or biphasic type, allowing the use of traditional rectangular or non-rectangular shapes [28].

A safety check is implemented in the interface to prevent the selection of stimulation parameters that fall outside the allowed protocol range. Furthermore, the interface allows the selection of the stimulation channels to be used.

The second window allows the use of stimulation algorithms based on linear modulation of amplitude, duration, or frequency. Stimulation can be modulated by using a ramp or trapezoidal profile. The third window allows psychophysical algorithms (i.e., rump-up until detection method [17], [23] and 1 up 2 down staircase procedure [39]) to be used for the automatic search of the stimulation threshold, allowing the user to select the number of reversals to be used to determine the threshold and the size of the steps to be used.

B. Benchtop Validation

Bench validation assessed current amplitude accuracy and independent programmability of multiple stimulation channels.

1) Experimental setup: To evaluate the stimulation performance of the device, a testing setup was designed comprising the following components: the proposed stimulator with its control GUI, a commercial benchtop stimulator with its control

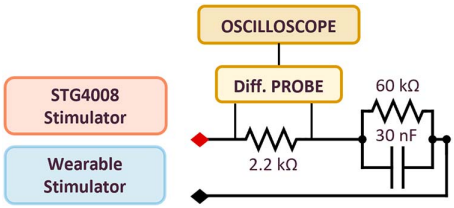

Fig. 3. Experimental bench setup for validating the stimulation performance of the proposed device in comparison with a benchmark stimulator, using a skin-like RC load.

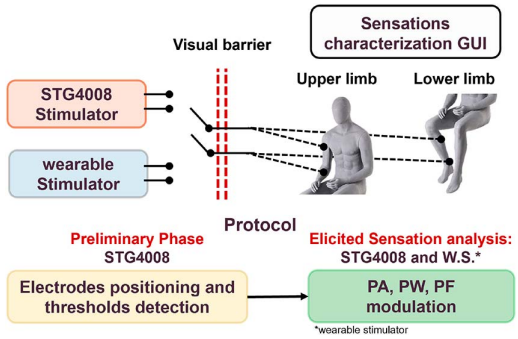

Fig. 4. The experimental setup used for tests with healthy participants. The operator controlled the stimulation parameters and selected which of the two devices to activate. A visual barrier was employed to ensure participant blinding. The lower part of the figure illustrates the two phases of the protocol and indicates the corresponding device used in each phase.

software, an oscilloscope (Teledyne T3DSO1202A, 200 MHz, CA, USA), and a differential probe (Pico Technology TA043, 100 MHz, TX, USA). The STG4008 benchtop stimulator, used as a benchmark in this study, is a fully programmable device controlled via dedicated software (MC Stimulus II). It has been employed in previous research involving SSF stimulation in both healthy and amputee subjects, [8], [17], [25], [26].

To simulate a skin-like load, two 5% tolerance resistors, 2.2-60 $k\Omega$, and a 30 nF capacitor, were used as illustrated in Fig. 3, [33].

2) Experimental protocol: To evaluate the current range and modulation step of the proposed stimulator, a set of stimulation waveforms was applied to an RC skin-like load

The actual current amplitude was determined by measuring the voltage across the 2.2 $k\Omega$ resistor, driven by the stimulation, and was then compared to the intended value.

To test the stimulator PA range, 10 current values were applied to the load, ranging from 1 mA to 10 mA by step of 1 mA.

Instead, to test the wearable stimulator PA resolution, 11 current values were delivered, ranging from 9 to 10 mA in 0.1 mA steps.

This high-amplitude range was specifically chosen to test the resolution of the device under stress conditions involving elevated charge delivery.

The PF and PW were set to the maximum values supported by the developed stimulator (500 Hz and 500 µs, respectively), with the stimulation duration set to 1 s. For each stimulus delivered, it was verified that there were no offsets, and the PA was measured for each of the 500 pulses.

These tests were conducted using both the developed and the benchmark stimulators. The percentage error between the desired and measured current for both stimulators was calculated as follows:

$$\text{Percentage error} = \left| \frac{\text{Measured current} - \text{Desired current}}{\text{Desired current}} \right| \times 100. \quad (2)$$

Measurement errors exceeding 5% were attributed to limitations in stimulator performance rather than resistor tolerance.

A second bench test was performed to demonstrate the feasibility of concurrent stimulation using two independent channels. During the experiment, both channels were simultaneously activated on separate skin-like loads, and the resulting waveforms were acquired and analyzed with an oscilloscope. Each channel was configured with a distinct set of stimulation parameters, ensuring no overlap between them.

The stimulation parameters defined for each channel are listed below.

- Ch.1: PA = 10 mA, PF = 400 Hz, PW = 400 us;
- Ch.2: PA = 6 mA, PF = 500 Hz, PW = 500 us.

To further investigate potential crosstalk effects between active channels, three additional benchtop tests were performed. Channel 2 was held at a fixed configuration (6 mA, 500 µs, 500 Hz), while each test independently modulated one stimulation parameter on Channel 1: (i) PA was varied from 10 to 4 mA, (ii) PW from 100 to 500 µs, and (iii) PF from 200 to 500 Hz. All waveforms were delivered concurrently through skin-like RC loads.

C. Human Validation

1) Experimental setup: The human validation aimed to assess the ability of the proposed stimulator to evoke somatotopic sensations in both upper and lower limbs. Participant responses were compared to those elicited in the same individuals using the STG4008 stimulator.

The study was approved by the Ethics Committee of University of Cagliari (ID:0191672) in compliance with the Declaration of Helsinki and its subsequent amendments. Twelve healthy participants were recruited for the study.

Ten participants (2 men and 8 women, aged 27 ± 1 years) were assigned to the upper limb group and ten participants (4 men and 6 women, aged 28 ± 2 years) were assigned to the lower limb group. The study objectives and procedures were clearly explained to the participants in accessible language, and all participants provided written informed consent.

The experimental setup is illustrated in Fig. 4.

Participants' somatotopic sensory responses were elicited using both the developed stimulator and the STG4008, along with their respective control software.

Participants were instructed to sit comfortably, with the target limb either resting on a table (upper limb) or suspended freely (lower limb).

TABLE II
RANGE AND MODULATION STEPS OF THE STIMULATION PARAMETERS ADOPTED DURING HEALTHY PARTICIPANTS PERCEIVED SENSATION TESTING

PA	PW	PF
PA = PA_{min}:0.1:PA_{Max} mA; PW = 500 μs; PF = 500 Hz;	PA = PA_{Max} mA; **PW** = 60:60:500 μs; PF = 500 Hz;	PA = PA_{Max} mA; PW = 500 μs; **PF** = 60:60:500 Hz;

Two circular, Ag/AgCl self-adhesive surface electrodes (25 mm diameter, TensCare Ltd, Epsom, UK) were placed either on the arm to stimulate the median nerve or on the leg to stimulate the tibial nerve. The median and tibial nerves were selected because they primarily innervate most of the hand and the foot, respectively.

Two graphical interfaces: the former for the upper limb and the latter for the lower limb, previously developed and validated in [21], [26], were used to record participants' responses during the stimulation sessions. These interfaces allowed participants to evaluate and specify the naturalness, depth, quality, and intensity of the elicited sensations.

Naturalness was categorized into five levels, namely: unnatural, almost unnatural, likely, almost natural, and natural.

Perceived stimulus depth was categorized as superficial, deep, or mixed.

Sensation quality was assessed by having participants classify each stimulus using one of thirteen predefined qualitative descriptors namely touch/pression, tingling, vibration, pinch, tug, burning, nothing, cold, hot, wrist flexion, finger flexion, wrist extension, finger extension.

Finally, the perceived intensity of the stimulus was rated on a scale from 0 to 10, with 0 indicating no sensation and 10 representing the maximum perceived intensity.

2) Experimental protocol: Human validation protocol was composed of two phases, a preparatory one followed by the evoked sensations characterization phase. After identifying the target limb, the first phase involved optimizing electrode placement over the median or tibial nerve and determining sensory and motor thresholds using the STG4008 stimulator. The benchmark device was employed in this phase to avoid potential limitations of the proposed system from influencing threshold identification. Sensory and motor thresholds were identified through a ramp-up procedure previously described in [23], [26], starting at 1 mA and increasing in 0.2 mA steps. In this preliminary phase, the pulse width (PW) and pulse frequency (PF) were fixed at 500 μs and 500 Hz, respectively. The sensory threshold was defined as the minimum amplitude required to evoke a somatotopic sensation on the target limb, while the motor threshold corresponded to the maximum amplitude eliciting such sensation without causing muscular twitching.

In the second phase, three different modulations were performed, each targeting one of the main stimulation parameters, as reported in Table II.

A visual barrier was used to prevent the participant from identifying the active stimulator. The stimulation device, either the test or the benchmark unit, was selected in a pseudo-randomized order by manually short-circuiting it through a shared breadboard, which also hosted the electrode leads.

After each stimulus, participants were asked to describe the perceived sensation in terms of quality, intensity, depth, naturalness, and location. Throughout the entire human validation protocol, stimulation duration was kept constant at 1 s.

3) Statistical analysis: Statistical analysis was performed to confirm the similarity between the results obtained from the proposed device and the benchmark.

To analyze the presence of statistically significant differences between the developed device and the benchmark stimulator at each modulation level, multiple Wilcoxon signed-rank tests were performed. Given the number of independent pairwise comparisons (n = 9) conducted within each scenario (stimulation parameter-target limb), a Bonferroni correction was applied to control for the increased risk of Type I error. Accordingly, the significance threshold was adjusted to $p < 0.0056$ (i.e., 0.05/9).

For the analysis of qualitative data, Cohen's kappa (k) was used to highlight the agreement index of the subject in perceiving the sensations elicited by the two stimulators as equivalent [8]. For k values between 0.8 and 1, there is near-perfect agreement between the sensations elicited by the two stimulators in the same participant. All statistical analyses were performed using MATLAB R2022b (MathWorks, Natick, MA, USA).

III. RESULTS

A. Benchtop Validation Results

The bench tests enabled the evaluation of the stimulation characteristics of the proposed device on a skin-like resistive-capacitive load in comparison with the commercial stimulator STG4008. Fig. 5 illustrates both the results of the tests conducted to evaluate the stimulation range and those assessing the modulation steps of the Pulse Amplitude parameter.

The errors of the wearable stimulator are represented in blue, while those of the benchmark are shown in red. In all the conducted tests, the proposed device successfully delivered stimulation currents with an error of less than 5%.

Fig. 6 shows oscilloscope recordings from two stimulation channels of the wearable device operating concurrently, each programmed with an independent set of stimulation parameters.

In this test, both outputs were delivered to the same skin-like resistive-capacitive load used in previous experiment.

The results confirm that the system can reliably deliver simultaneous stimulation through two independently programmed channels, with no evidence of parameter interference. In all tests, deviations from the target values remained within $\pm 2\%$, demonstrating the absence of cross-talk and ensuring consistent, independent modulation across channels.

B. Human Validation Results

Both electrical stimulators were randomly interleaved to stimulate the upper and lower limbs of healthy participants through experimental tests, leading to three types of data collection: perceived stimulus intensity, qualitative evaluation of the evoked sensations, and analysis of the stimulated areas. Each

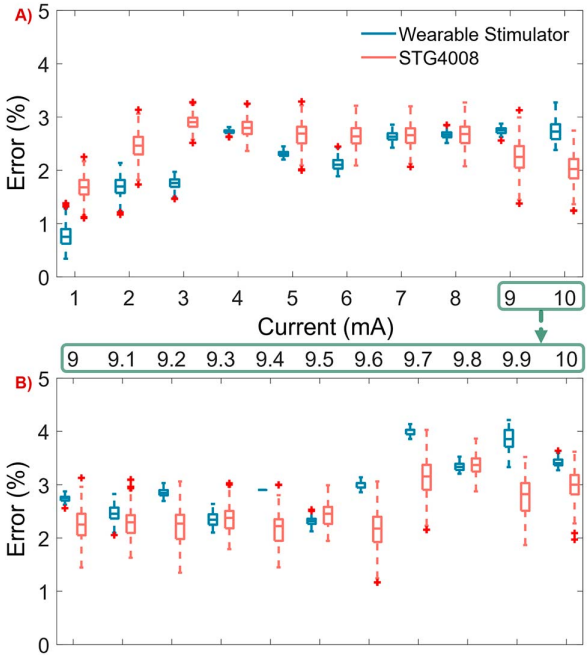

Fig. 5. Percentage errors in the output current amplitudes generated by the wearable stimulator (blue) and the benchmark STG4008 (red). Panel A) shows the errors measured during the stimulation range test, while Panel B) reports those obtained from the modulation step test of the pulse amplitude parameter.

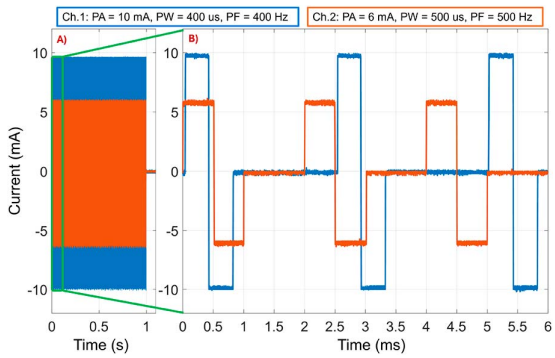

Fig. 6. (A) Simultaneous activation of channels 1 and 2, each delivering a one-second pulse train. (B) Close-up view illustrating the different stimulation sets used for the two channels.

result includes the outcomes of both frequency and charge modulation, the latter obtained by combining data from PA and PW modulations. While changes in stimulation frequency affect the total injected charge over time, in this work, charge modulation specifically refers to the charge delivered per individual pulse, as determined by variations in PA and PW.

1) Perceived Intensity: The intensity of the stimuli perceived by participants during the experimental tests is shown in Fig. 7. Specifically, Fig. 7A and Fig. 7B present the results of the frequency and charge modulation tests for the upper limb, respectively, while Fig. 7C and Fig. 7D display the corresponding results for the lower limb.

The yellow and blue boxplot represent the results from the wearable stimulator for the upper and lower limbs, respectively, while the black and red bars correspond to the STG4008 results for the upper and lower limbs.

No statistically significant differences were observed between the intensities elicited by the developed stimulator and the benchmark for all case studies.

In the frequency modulation tests, a clear relationship is observed between the increase in stimulus frequency and the corresponding rise in perceived intensity, for both stimulated limbs. At each frequency, the stimulus applied to the lower limb was perceived with greater median intensity compared to the upper limb.

In the charge modulation tests, the perceived stimulus intensity directly increases with the modulation parameter, whether it is PW or PA. In order to perceive the same level of intensity, a higher amount of charge is required for the lower limb.

2) Evoked sensations quality: The stacked bar plots in Fig. 8 provide a simplified visual comparison of the qualities of sensations elicited in participants by the two stimulators. The chart displays both upper and lower limb results.

For each limb, the characterizations of naturalness (orange shade), depth (yellow shade), and quality (green shade) of the elicited sensations are presented.

Additionally, for each characterization, the results from both frequency modulation and charge modulation tests are shown, with stimuli delivered by both the developed stimulator and the STG4008. The benchmark results can be distinguished by the dotted texture. Each bar plot represents the percentage of times a sensation was characterized in a specific way relative to the total number of tests.

Cohen's K coefficient was used to evaluate the level of agreement between the sensations elicited by the two devices.

All k values exceed 0.9, indicating a high degree of agreement of the participants in classifying the stimuli received by the two stimulators.

Up to 90% of the stimuli were perceived as superficial in both limbs and modulations. Charge modulation resulted in more natural sensations overall than frequency modulation. Although this pattern exists in both limbs, it is particularly noticeable in the upper one where sensations are described as "almost natural" (59% with the developed stimulator and 63% with STG4008) when it comes to charge modulation and "almost unnatural" (53% with the stimulator and 54% with STG4008) when it comes to frequency modulation.

Tingling and vibration are the mostly elicited qualities. For both the stimulated limb, from 75% to 90% of the "quality typology" choices are represented by them.

Frequency modulation consistently elicited perceptible sensations, whereas charge modulation resulted in 19% and 15% of stimuli being reported as "no sensation" in the upper and lower limb tests, respectively. Finally, pinch sensations were elicited mostly in the lower limb through frequency modulation, up to 15%.

3) Elicited areas: Volunteers used the graphical user interfaces to map the elicited areas on the hand or foot after each stimulus. To examine how these areas change varying the stimulation parameters, two types of analyses were conducted.

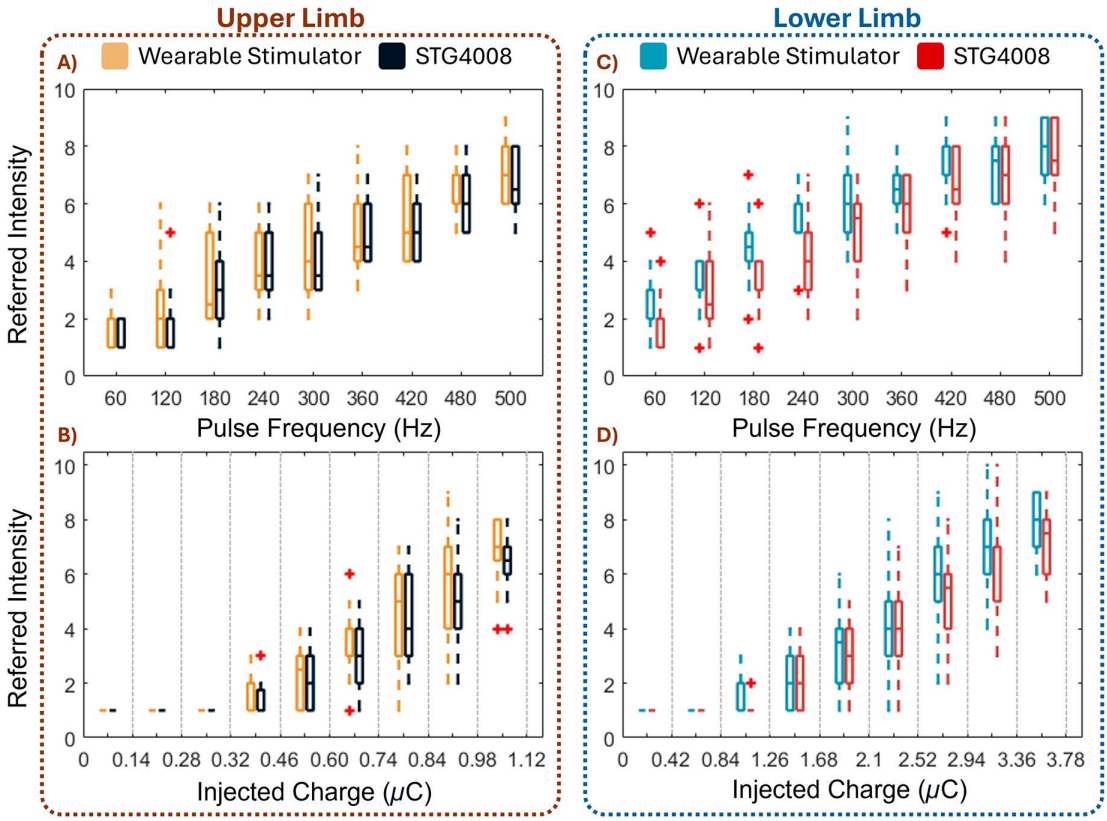

Fig. 7. Stimuli perceived intensity reported by participants during frequency modulation for the A) upper limb and C) lower limb, and during charge modulation for the B) upper limb and D) lower limb. The analysis was performed using both the STG4008 and the proposed stimulator. The + sign indicates the outlier. No statistically significant difference (Wilcoxon ranksum test whit bonferroni correction, P<0.0056) are reported.

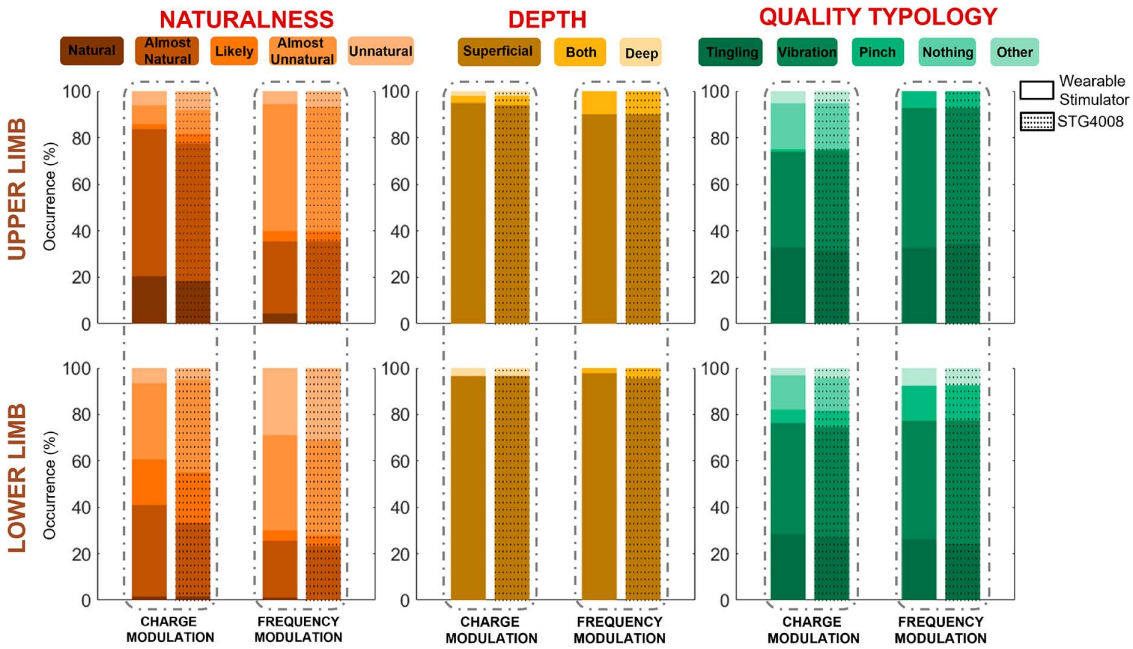

Fig. 8. Classification of the qualities elicited by the stimulators during the perceived sensations tests. For each limb, the naturalness, depth, and quality of the sensations perceived by the participants are reported. The results of the charge and frequency modulation for both stimulators are provided for each class. The dot texture distinguishes the results obtained with the STG4008.

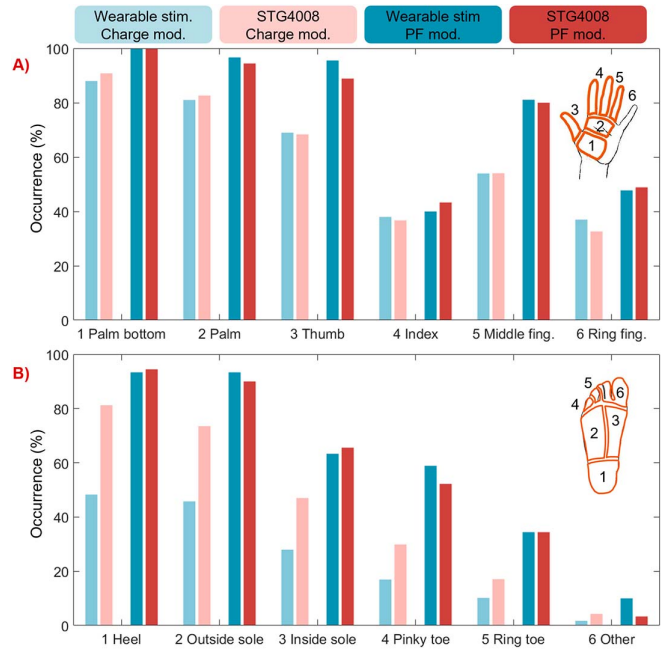

Fig. 9. Occurrences of stimulation targeting specific regions of the hand (A) or foot (B) delivered by either the wearable stimulator (blue) or the benchmark device (red). Lighter color pairs correspond to data from charge modulation tests, while darker pairs represent results from frequency modulation tests. Each graph includes the applied mask, divided into six distinct regions, used to discretize and analyze the areas of the hand or foot under investigation.

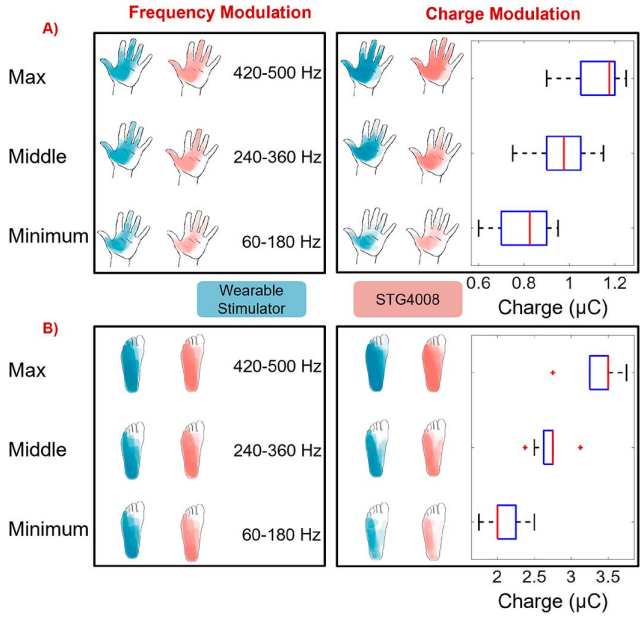

Fig. 10. Variation in the stimulated surface area of the hand (A) and foot (B) using both the wearable stimulator (blue) and the benchmark (red) across two modulation tests. For each modulation, the stimulated areas were divided into three equally sized groups. Within each group, all reported areas were superimposed to create a single image, where darker regions represent areas of greater stimulation. Additionally, the range of the corresponding modulation parameter is specified for each group. The + sign highlights the outlier.

The first analysis, shown in Fig. 9, focused on local variations in the elicited areas. One mask was generated for each limb surface to divide the hand and foot into six distinct regions.

By intersecting these masks with the participant-drawn elicited areas, the number of times each region was evoked out of the total number of stimuli was determined. Fig. 9A presents the results from the upper limb tests, while Fig. 9B depicts the results from the lower limb tests. In both graphs the results obtained with the benchmark stimulator are shown in red, while those obtained with the presented device are shown in blue.

Light-colored bars indicate the results of the charge modulation tests, while dark-colored bars represent those from the frequency modulation tests. Frequency modulation in both limbs enabled the simultaneous stimulation of a higher number of zones compared to charge modulation.

In all cases, the stimuli are perceived with a higher occurrence in the proximal regions, as these areas are the first to be stimulated with lower injected charges and remain stimulated even as the injected charge increases.

For the upper limb, the results obtained using the developed stimulator and the benchmark are comparable. In the lower limb, frequency modulation results are consistent between the two devices; however, charge modulation occurrences differ. Specifically, during charge modulation, the proposed device stimulated a smaller area of foot with respect to the STG4008.

The second analysis, shown in Fig. 10, illustrates the global distribution of elicited areas across three modulation levels: Minimum, Middle, and Max each comprising an equal number of trials.

For each subset, the elicited areas were overlaid to produce a single image where darker regions represent the areas most frequently stimulated. The areas stimulated by the proposed device are indicated in blue, while those stimulated by the benchmark are shown in red. For each subset, the corresponding ranges of the modulated parameter values are also provided. In all experimental conditions, the stimulated areas of the hand and foot increased proportionally with higher values of the modulated stimulation parameter.

The most frequently activated areas, represented by the darkest regions, correspond to the anatomical district innervated by the median nerve in the hand and the tibial nerve in the foot, which were specifically targeted during the tests. In all reported cases, the areas activated by the two stimulators are consistent in both extent and shade.

To enable a more objective analysis of the stimulation areas obtained using the developed device and the benchmark, the Structural Similarity Index Measure (SSIM) was computed [21], [40]. Specifically, SSIM was applied to all pairs of stimulation areas, reported in Fig. 10, elicited by the two devices under identical stimulation conditions. For all analyzed pairs, the SSIM index exceeded 0.9, indicating a high degree of similarity between the stimulation areas elicited by the two devices.

IV. Discussion

A comparative analysis with wearable devices from literature and commercial sources (Table III) confirms that the proposed system meets standard wearability criteria in terms of size and weight. Moreover, the device offers key advantages such

TABLE III
COMPARISON OF THE MAIN WEARABILITY FEATURE BETWEEN THE PROPOSED DEVICE AND OTHER RESEARCH GRADE, COMMERCIAL WEARABLE STIMULATORS

Reference	Dimensions (mm)	Mass (g)	Power Consumption (mW)
This work	70x40x35	64	1300
[29]	40x42x26	42	N.A.
[30]	50x73x32	280	N.A.
[35]	59x56	N.A.	N.A.
[36]	70x50x1.6	52	N.A.

N.A: Not Available.

as multi-channel programmability and adaptability for TENS-based SSF in both upper and lower limbs, features not simultaneously available in other systems.

Bench tests validated the device capability to deliver pulse amplitude within the required range (1–10 mA) and resolution (0.1 mA) on skin-like RC loads, as needed to elicit different somatotopic sensation in both healthy and amputee subjects. Oscilloscope recordings (Fig. 6) confirmed the ability to generate two concurrent and independently parameterized stimulation waveforms, demonstrating true multi-channel capability.

Tests conducted on healthy participants yielded results consistent with other prior SSF studies [17], [21] and no statistically significant differences were observed between the developed and benchmark stimulator across all measured metrics.

Additionally, the interchangeability coefficient (k) consistently exceeded 0.9 across all analyzed cases. The results demonstrate that the wearable stimulator elicited somatotopic sensations equivalent to those produced by the benchmark device, both in terms of perceived intensity and qualitative characteristics. These findings confirm the functional equivalence of the two systems and support the proposed stimulator as a viable platform for delivering TENS-based somatotopic sensory feedback.

Frequency modulation tests revealed greater perceived intensity in the lower limb compared to the upper limb (Fig. 7), potentially due to differences in the naturalness of the evoked sensations. Sensations perceived as less natural, as observed in the lower limb tests (Fig. 8), tend to be experienced as more intense.

Some stimuli, delivered by both devices, failed to elicit any sensation during the charge modulation tests due to the use of excessively low pulse width values, which limited the total delivered charge. This limitation was slightly more evident in the upper limb (19% upper vs 15% lower), despite the median charge required to elicit a perceptible sensation being significantly lower for the hand (0.85 μC) compared to the foot (2 μC).

The proposed device elicited more spatially localized responses during lower limb charge modulation tests (Fig. 9), likely due to reduced maximum deliverable charge compared to the benchmark. Conversely, in frequency modulation tests, identified as the most effective for eliciting somatotopic sensations across broader skin areas, the stimulation areas elicited by both devices were comparable, both locally (Fig. 9) and globally (Fig. 10).

The device successfully elicited somatotopic sensations in both upper and lower limbs, consistent with the benchmark stimulator and existing literature. While validation was limited to healthy participants, stimulation parameter design was derived from studies including both able-bodied and amputee populations. Nevertheless, further validation on amputee participants will be necessary to confirm its effectiveness.

V. CONCLUSION

This work presented a wearable TENS stimulator designed to deliver somatotopic sensory feedback to both upper and lower limbs. The system was evaluated via bench testing and validated with healthy participants, using a commercial stimulator as benchmark. Key metrics included perceived quality, intensity, and spatial localization of the evoked sensations.

The proposed stimulator elicited sensations comparable to the benchmark, with no statistically significant differences between the two devices.

Overall outcomes were consistent with prior somatotopic studies, with the stimulated areas corresponding to the ones innervated by the median and tibial nerve.

The proposed device represents a practical alternative to conventional benchtop stimulators commonly used in TENS-SSF research, offering both wearability and adequate stimulation capabilities.

Future work will aim to integrate the device into a prosthetic system to enable closed-loop control and to validate its effectiveness in amputee participants.

ACKNOWLEDGMENT

Views and opinions expressed are however those of the authors only and do not necessarily reflect those of the European Union or European Commission. Neither the European Union nor the granting authority can be held responsible for them.

ETHICAL STATEMENT

The authors assert that all procedures contributing to this work comply with the ethical standards of the relevant national and institutional committees and with the Helsinki Declaration of 1975, as revised in 2008.

All participants provided informed consent before participating in the study. The experiments were approved by the Ethics Committee of the University of Cagliari under prot. n.1091672

REFERENCES

[1] L. E. Fisher, R. A. Gaunt, and H. Huang, "Sensory restoration for improved motor control of prostheses," *Current Opin. Biomed. Eng.*, vol. 20, 2023, Art. no. 100498.
[2] S. Raspopovic, G. Valle, and F. M. Petrini, "Sensory feedback for limb prostheses in amputees," *Nat. Mater.*, vol. 20, no. 7, pp. 925–939, 2021.
[3] L. E. Osborn et al., "Prosthesis with neuromorphic multilayered e-dermis perceives touch and pain," *Sci. Robot.*, vol. 3, no. 19, 2018, Art. no. eaat3818.
[4] E. D'anna et al., "A somatotopic bidirectional hand prosthesis with transcutaneous electrical nerve stimulation based sensory feedback," *Sci. Rep.*, vol. 7, no. 1, 2017, Art. no. 10930.

[5] F. M. Petrini et al., "Sensory feedback restoration in leg amputees improves walking speed, metabolic cost and phantom pain," *Nat. Med.*, vol. 25, no. 9, pp. 1356–1363, 2019.
[6] H. Charkhkar, C. E. Shell, P. D. Marasco, G. J. Pinault, D. J. Tyler, and R. J. Triolo, "High-density peripheral nerve cuffs restore natural sensation to individuals with lower-limb amputations," *J. Neural Eng.*, vol. 15, no. 5, 2018, Art. no. 056002.
[7] S. Raspopovic et al., "Restoring natural sensory feedback in real-time bidirectional hand prostheses," *Sci. Transl. Med.*, vol. 6, no. 222, p. 222ra19, 2014.
[8] L. Vargas, G. Whitehouse, H. Huang, Y. Zhu, and X. Hu, "Evoked haptic sensation in the hand with concurrent non-invasive nerve stimulation," *IEEE Trans. Biomed. Eng.*, vol. 66, no. 10, pp. 2761–2767, Oct. 2019.
[9] L. Vargas, H. Huang, Y. Zhu, and X. Hu, "Object shape and surface topology recognition using tactile feedback evoked through transcutaneous nerve stimulation," *IEEE Trans. Haptics*, vol. 13, no. 1, pp. 152–158, Jan./Mar. 2020.
[10] H. Charkhkar, B. P. Christie, and R. J. Triolo, "Sensory neuroprosthesis improves postural stability during sensory organization test in lower-limb amputees," *Sci. Rep.*, vol. 10, no. 1, 2020, Art. no. 6984.
[11] F. M. Petrini et al., "Enhancing functional abilities and cognitive integration of the lower limb prosthesis," *Sci. Transl. Med.*, vol. 11, no. 512, 2019, Art. no. eaav8939.
[12] C. Günter, J. Delbeke, and M. Ortiz-Catalan, "Safety of long-term electrical peripheral nerve stimulation: review of the state of the art," *J. NeuroEng. Rehabil.*, vol. 16, no. 13 pp. 16:1–16, Jan. 2019.
[13] M. Gonzalez, A. Bismuth, C. Lee, C. A. Chestek, and D. H. Gates, "Artificial referred sensation in upper and lower limb prosthesis users: A systematic review," *J. Neural Eng.*, vol. 19, no. 5, 2022, Art. no. 051001.
[14] C. Pasluosta, P. Kiele, and T. Stieglitz, "Paradigms for restoration of somatosensory feedback via stimulation of the peripheral nervous system," *Clin. Neurophysiol.*, vol. 129, no. 4, pp. 851–862, 2018.
[15] L. Chee, G. Valle, G. Preatoni, C. Basla, M. Marazzi, and S. Raspopovic, "Cognitive benefits of using non-invasive compared to implantable neural feedback," *Sci. Rep.*, vol. 12, no. 1, 2022, Art. no. 16696.
[16] V. Bucciarelli et al., "Multiparametric non-linear tens modulation to integrate intuitive sensory feedback," *J. Neural Eng.*, vol. 20, no. 3, 2023, Art. no. 036026.
[17] A. Scarpelli et al., "Eliciting force and slippage in upper limb amputees through transcutaneous electrical nerve stimulation (TENS)," *IEEE Trans. Neural Syst. Rehabil. Eng.*, vol. 32, pp. 3006–3017, 2024.
[18] M. Li et al., "Discrimination and recognition of phantom finger sensation through transcutaneous electrical nerve stimulation," *Front. Neurosci.*, vol. 12, 2018, Art. no. 283.
[19] J. Zhang et al., "Evaluation of multiple perceptual qualities of transcutaneous electrical nerve stimulation for evoked tactile sensation in forearm amputees," *J. Neural Eng.*, vol. 19, no. 2, 2022, Art. no. 026041.
[20] L. Vargas, H. Shin, H. Helen Huang, Y. Zhu, and X. Hu, "Object stiffness recognition using haptic feedback delivered through transcutaneous proximal nerve stimulation," *J. Neural Eng.*, vol. 17, no. 1, 2019, Art. no. 016002.
[21] A. Demofonti, A. Scarpelli, F. Cordella, and L. Zollo, "Modulation of sensation intensity in the lower limb via transcutaneous electrical nerve stimulation," in *Proc. 43rd Annu. Int. Conf. IEEE Eng. Med. Biol. Soc. (EMBC)*, Piscataway, NJ, USA: IEEE Press, 2021, pp. 6470–6474.
[22] L. Pan, L. Vargas, A. Fleming, X. Hu, Y. Zhu, and H. H. Huang, "Evoking haptic sensations in the foot through high-density transcutaneous electrical nerve stimulations," *J. Neural Eng.*, vol. 17, no. 3, 2020, Art. no. 036020.
[23] A. Demofonti et al., "Somatotopical feedback restoration in the lower limb through tens: A feasibility study," *Convegno Nazionale di Bioingegneria*, pp. 198–201, 2020.
[24] A. Demofonti et al., "Restoring somatotopic sensory feedback in lower limb amputees through non-invasive nerve stimulation," *Cyborg Bionic Syst.*, vol. 6, Apr. 2025.
[25] H. Shin, Z. Watkins, H. Helen Huang, Y. Zhu, and X. Hu, "Evoked haptic sensations in the hand via non-invasive proximal nerve stimulation," *J. Neural Eng.*, vol. 15, no. 4, 2018, Art. no. 046005.
[26] A. Scarpelli, A. Demofonti, F. Terracina, A. L. Ciancio, and L. Zollo, "Evoking apparent moving sensation in the hand via transcutaneous electrical nerve stimulation," *Front. Neurosci.*, vol. 14, 2020, Art. no. 534.
[27] G. Chai, X. Sui, S. Li, L. He, and N. Lan, "Characterization of evoked tactile sensation in forearm amputees with transcutaneous electrical nerve stimulation," *J. Neural Eng.*, vol. 12, no. 6, 2015, Art. no. 066002.
[28] R. Collu, E. J. Earley, M. Barbaro, and M. Ortiz-Catalan, "Non-rectangular neurostimulation waveforms elicit varied sensation quality and perceptive fields on the hand," *Sci. Rep.*, vol. 13, no. 1, 2023, Art. no. 1588.
[29] H. Wang, G. Chai, X. Sheng, and X. Zhu, "A programmable, multi-channel, miniature stimulator for electrotactile feedback of neural hand prostheses," in *Proc. 10th Int. IEEE/EMBS Conf. Neural Eng. (NER)*, Piscataway, NJ, USA: IEEE Press, 2021, pp. 1026–1029.
[30] HASOMED, RehaMove3. Magdeburg, Germany. [Online]. Available: https://hasomed.de/produkte/rehamove/
[31] C. Basla, L. Chee, G. Valle, and S. Raspopovic, "A non-invasive wearable sensory leg neuroprosthesis: Mechanical, electrical and functional validation," *J. Neural Eng.*, vol. 19, no. 1, 2022, Art. no. 016008.
[32] A. N. Collimore et al., "A portable, neurostimulation-integrated, force measurement platform for the clinical assessment of plantarflexor central drive," *Bioengineering*, vol. 11, no. 2, 2024, Art. no. 137.
[33] S. I. Birlea, P. P. Breen, G. J. Corley, N. M. Birlea, F. Quondamatteo, and G. ÓLaighin, "Changes in the electrical properties of the electrode–skin–underlying tissue composite during a week-long programme of neuromuscular electrical stimulation," *Physiol. Meas.*, vol. 35, no. 2, 2014, Art. no. 231.
[34] R. Collu et al., "Wearable high voltage compliant current stimulator for restoring sensory feedback," *Micromachines*, vol. 14, no. 4, p. 782, 2023.
[35] M. A. Trout, A. T. Harrison, M. R. Brinton, and J. A. George, "A portable, programmable, multichannel stimulator with high compliance voltage for noninvasive neural stimulation of motor and sensory nerves in humans," *Sci. Rep.*, vol. 13, no. 1, 2023, Art. no. 3469.
[36] F. Mereu et al., "A sensory feedback neural stimulator prototype for both implantable and wearable applications," *Micromachines*, vol. 15, no. 4, p. 480, 2024.
[37] R. Collu, J. Fuentes, S. Sánchez, S. Lai, and M. Barbaro, "Development of an electrical current stimulator for activating muscle tissues in biohybrid machines," in *Proc. 46th Annu. Int. Conf. IEEE Eng. Med. Biol. Soc. (EMBC),* Piscataway, NJ, USA: IEEE Press, 2024, pp. 1–4.
[38] R. Collu et al., "Development of an electrical current stimulator for controlling biohybrid machines," *Sci. Rep.*, vol. 15, no. 1, 2025, Art. no. 22473.
[39] C. Kaernbach et al., "Simple adaptive testing with the weighted up-down method," *Perception & Psychophys.*, vol. 49, no. 3, pp. 227–229, 1991.
[40] L. E. Osborn et al., "Sensory stimulation enhances phantom limb perception and movement decoding," *J. Neural Eng.*, vol. 17, no. 5, 2020, Art. no. 056006.

Roberto Paolini was born in Teramo, Italy, in 1995. He received the M.Sc. degree in biomedical engineering from the University Campus Bio-Medico of Rome (UCBM), in 2021. He is currently working toward the Ph.D. degree with the Science and Engineering for Humans and the Environment, UCBM. His research interests include sensory feedback, wearable electrical stimulation devices, and neurostimulation of the peripheral nervous system.

Riccardo Collu was born in Cagliari, Italy, in 1996. He received the M.Sc. degree in electronic engineering from the University of Cagliari, in 2020, and the Ph.D. degree in electronic and computer engineering in 2024. He is an Assistant Professor with the Department of Electrical and Electronic Engineering, University of Cagliari. His current research interests include the design of CMOS implantable systems for neural interfaces and biomedical applications, wearable systems, and neurostimulation of peripheral nervous systems.

Laura Tullio received the B.S. degree in clinical engineering from Sapienza University of Rome, Italy, in 2021, and the M.S. degree in biomedical engineering from the University Campus Bio-Medico of Rome, Italy, in 2024. Her research focuses on robotics, mechatronics and neuroengineeering, with her thesis addressing the validation of a wearable TENS-based device to restore sensory feedback in limb amputees.

Andrea Demofonti (Member, IEEE) received the B.Sc. degree in industrial engineering, the M.Sc. in biomedical engineering, and the Ph.D. degree in science and engineering for humans and the environment from the Università Campus Bio-Medico di Roma (UCBM), Italy, in 2015, 2017, and 2022, respectively. He is currently a Postdoctoral Research Fellow with the Research Unit of Advanced Robotics and Human-centred Technologies and a Research Assistant with the Research Unit SYNERGIA, Centro Santa Maria della Provvidenza, IRCCS Fondazione Don Carlo Gnocchi. His current research interests include the design and development of systems for the upper and/or lower limb sensorimotor capabilities restoration via electric stimulation.

Alessia Scarpelli received the B.Sc. degree in industrial engineering and the M.Sc. degree in biomedical engineering from the Università Campus Bio-Medico di Roma (UCBM), Rome, Italy, in 2017 and 2019, respectively, and the Ph.D. degree in science and engineering for human and environment from UCBM, in 2024. She is currently a Postdoctoral Researcher with the Advanced Robotics and Human-Centred Technologies Research Unit, UCBM. Her research interests mainly include bionic systems and sensory feedback for upper-limb sensory-motor impairments.

Francesca Cordella (Member, IEEE) received the Laurea degree in electronic engineering and the Ph.D. degree in computer and automation engineering from the University of Naples Federico II. She is currently an Associate Professor of bioengineering with the Campus Bio-Medico University of Rome. She is a member of the Technical and Scientific Program Committee and an Associate Editor for several international conferences, workshops, and journals. She is a Co-Chair of the IEEE/RAS Technical Committee on Rehabilitation and Assistive Robotics. She was/is involved in the role of a Co-Principal Investigator, a Project Manager, and a Scientific Manager of Work Package for more than 25 European and national projects in her fields of interest. She has authored/coauthored 3 patents and more than 100 peer-reviewed publications appeared in international journals, books, and conference proceedings.

Massimo Barbaro (Senior Member, IEEE) was born in Cagliari, Italy, in 1972. He received the M.S. degree in electronic engineering and the Ph.D. degree in electronic and computer engineering from the University of Cagliari, Italy, in 1997 and 2001, respectively. Since 2002, he joined the Department of Electrical and Electronic Engineering, University of Cagliari, Italy, as an Assistant Professor, where he is currently a Full Professor of electronics. His research topics include smart sensors, smart agriculture, biosensors and implantable electronics for neural interfaces. For more information, see https://web.unica.it/unica/page/en/massimo_barbaro.

Loredana Zollo (Senior Member, IEEE) received the M.S. degree in electronic engineering from the Università degli Studi di Napoli Federico II, in 2000, and the Ph.D. degree in bioengineering from Scuola Superiore Sant'Anna di Pisa, in 2004. She is currently a Full Professor of bioengineering and the Director of the Master of Science in Biomedical, Università Campus Bio-Medico di Roma (UCBM), where she is also the Director of the CREO Lab-Laboratory of Advanced Robotics and Human-Centred Technologies. She has been involved in more than 40 EU-funded and national projects in her application fields, such as EU H2020/FET-Open/SOMA as a Project Coordinator and EU H2020/ODIN and AIDE as a Scientific Coordinator with UCBM. She has authored/coauthored more than 160 scientific publications and six patents. Her research interests include rehabilitation and assistive robotics, bio robotics and bionics, human–machine interfaces, and collaborative robotics.